Evidence of localized surface plasmon enhanced magneto-optical effect in nanodisk array

doi: 10.1063/1.3334726

Evidence of localized surface plasmon enhanced magneto-optical effect in nanodisk array

Guan Xiang Du,[1,a)] Tetsuji Mori,[2] Michiaki Suzuki,[1] Shin Saito,[1] Hiroaki Fukuda,[2] and Migaku Takahashi[1]

[1]*Department of Electronic Engineering, Graduate School of Engineering, Tohoku University, 6-6-05 Aoba, Aramaki, Aoba-ku, Sendai 980-8579, Japan*

[2]*Device and Module Technology Development Center, Corporate Technology Development Group, Ricoh Company, Ltd., 16-1 Shinei-Cho, Tsuzuki-ku, Yokohama 224-0035, Japan*

(Received 17 December 2009; accepted 29 January 2010; published online 25 February 2010)

Nanodisk array with sandwich structure of $Au/[Co/Pt]_n/Au$ was fabricated by electron beam lithography combined with argon ion milling. Excitation of localized surface plasmon resonance (LSPR) was demonstrated for various disk diameters. Magneto-optical (MO) properties were measured by a home-made micro-Faraday system at wavelengths of 633 and 690 nm. Faraday ellipticity at 690 nm showed non-monotonic dependence on disk diameter and reached maximum for disk diameter of 84 nm, which was associated with LSPR at 690 nm. The experimental results show direct evidence for LSPR enhancement effect on MO properties. The optical and MO properties were fitted by average field approximation. © *2010 American Institute of Physics*. [doi:10.1063/1.3334726]

During the past two decades, tremendous progress has been made in the development of various applications based on surface plasmon resonance (SPR) and localized surface plasmon resonance (LSPR) in noble metal nanostructures.[1–3] Refractometry in bio/chemical sensing[4] was based on the ultrahigh sensitivity of SPR/LSPR on the refractive index of surrounding dielectrics. LSPR has also been widely used to increase the efficiency of photoemission in light emitting diodes,[5] conversion efficiency of solar cells,[6] and fluorescence.[7] In the study of magneto-optical (MO) effect, two-dimensional multilayer structure of M/MO/M/dielectrics in Kretschmann configuration has been studied, where M is noble metals such as Au and Ag.[8–10] It has been well established that the resonance behavior of the MO effect is originated from the presence of propagating SPR. However, it was only recently recognized that the MO effect might also be enhanced by LSPR in nanostructures.[11–13] One of the important and fundamental challenges is to combine both noble metal and MO materials into nanostructures. Recently, nanosphere lithography was applied to pattern Au/Co/Au films into nanosandwiches by using polystyrene spheres as etching mask.[11] In another work, suspension of gold coated iron oxide core-shell nanostructures was synthesized by colloidal method.[12] In both works, the authors pointed out LSPR enhancement on MO effect by associating the spectral characteristics of optical properties with MO properties. However, to further investigate the LSPR effect on the MO effect, precise control of size, shape, and arrangement of nanostructures is indispensible since these factors sensitively modify the spectral characteristics of LSPR in nanostructures. Electron beam lithography (EBL) combined with ion milling proves to be a suitable tool for this purpose. It is noteworthy that, since it is very time-consuming and unpractical for this method to fabricate large-area samples, a micro-Faraday system equipped with objective lens design as well as laser source was constructed to measure micrometer-scaled samples (10^4 μm^2).

In this work, the authors presented the optical and MO properties of nanodisk square array consisting of sandwich structure of $Au/[Co/Pt]_n/Au$. Thin film with stacking structure of $Ti(2)/Au(20)/Pt(1)/[Co(0.5)/Pt(1)]_7/Au(20)$ (unit: nm) was deposited on glass substrate with Ti buffer layer by dc sputtering, wherein multilayer of $[Co/Pt]_n$ possessed perpendicular anisotropy. Argon ion milling was used to transfer nanodisk pattern formed by negative resist TGMR (TOK Co., Ltd.). Followed by the ion milling process, a layer of resist with thickness of 150 nm was spin-coated on the sample surface. Layout of the nanodisk array was described by both grating constant (h) and disk diameter (d). Throughout this work h was fixed to 250 nm. Typical scanning electron microscope (SEM) image of nanodisk array (d=84 nm) was shown in Fig. 1(b2). Sidewall redeposits

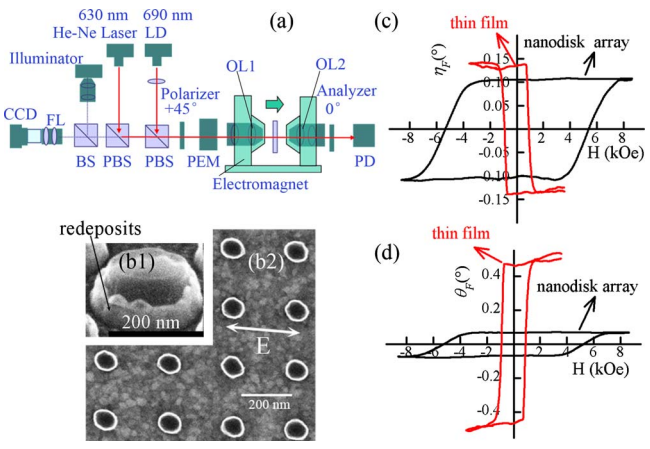

FIG. 1. (Color online) (a) Illustration diagram of the home-made micro-Faraday measurement system. Typical SEM images for sidewall redeposits (b1) and nanodisk array (b2), wherein double-ended arrow refers to the polarization plane. (c) Ellipticity and (d) rotation angle loops at 690 nm for thin film and nanodisk array (d=84, h=250 nm). Ellipticity for thin film is negative while positive for nanodisk array.

[a)]Electronic mail: gxdu@ecei.tohoku.ac.jp.

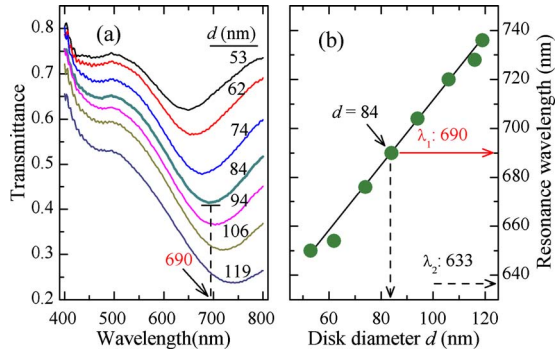

FIG. 2. (Color online) Optical properties. (a) Transmittance spectra of nanodisk array with various disk diameters d, wavelength at minimum for each curve corresponds to spectral location of LSPR. Particularly, resonance wavelength for array with d of 84 nm (thick line) is 690 nm. (b) Dependence of resonance wavelength on disk diameter. Arrows show the two measurement wavelengths 690 and 633 nm, respectively.

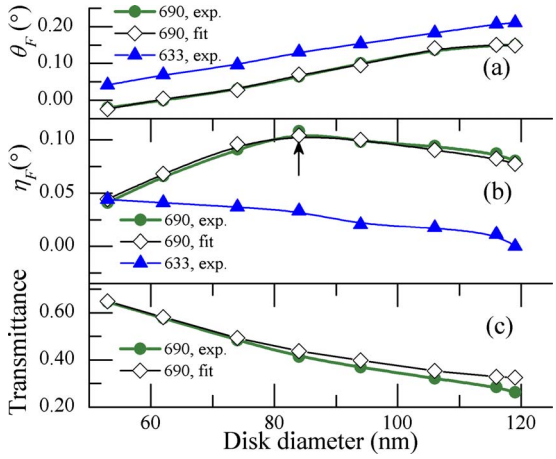

FIG. 3. (Color online) (a) Rotation angle, (b) ellipticity, and (c) transmittance of nanodisk array at wavelengths of 630 and 690 nm as a function of disk diameter. Solid circle and solid triangle refer to experimental data measured at wavelengths of 690 and 633 nm, respectively; empty diamond refers to fitting data for 690 nm. Arrow in (b) marks peak of η_F at d=84 nm (measured at λ=690 nm).

surrounding the nanodisks were observed as shown in Fig. 1(b1). Chip size of the array was 150×150 μm^2. Transmittance spectra of the nanodisk array were measured by microspectrometer with objective lens numerical aperture of 0.13 to exclude any spurious light. MO properties were measured in a home-made micro-Faraday measurement system. Light beam was normally incident on the samples, magnetic field was applied along the light propagation direction, two laser wavelengths of 633 (He-Ne laser) and 690 nm (laser diode) were used in this study. The illustration diagram of the measurement system was shown in Fig. 1(a). For both optical and MO properties measurement, polarization plane of incident light was along the axis connecting the nearest-neighbor disks as indicated by the double-ended arrow in Fig. 1(b2). Typical Faraday rotation angle (θ_F) and ellipticity (η_F) loops measured at laser wavelength of 690 nm were shown in Figs. 1(c) and 1(d), respectively. Compared to continuous thin film, nanodisk array (d=84 nm) showed increased coercivity. The magnitude of ellipticity for nanodisk array was comparable to that of thin film even though the volume fraction ($0.25\pi d^2/h^2$) of MO materials in nanodisk array was less than 9%. Moreover, ellipticity for nanodisk array was positive (+0.11°) while that for thin film changed to negative (−0.14°).

To understand the observed intriguing difference of MO properties between thin film and nanodisk array, various disk sizes were investigated. First, transmittance spectra at wavelengths of 400–800 nm were measured for disk sizes ranging from 53 to 119 nm as shown in Fig. 2(a). Transmittance minimum on each curve was due to excitation of LSPR which resulted in enhanced optical extinction cross section. Resonance wavelength (λ_R) as a function of disk diameter was summarized in Fig. 2(b). λ_R ranged from 650 to 736 nm. The redshift of λ_R with increasing disk diameter was attributed to both shape and retardation effect.[14] To investigate the MO properties under resonance condition, the measurement wavelength was chosen to be 690 nm (λ_1) so that it was located in the range of 650–736 nm. Especially, λ_R for d of 84 nm was nearly 690 nm as indicated by the arrow in Fig. 2(a). To be noted is that, it was unpractical to evaluate the spectral properties for nanodisk array. To investigate the role of LSPR on the MO effect, we chose one or two laser wavelengths and by varying the disk size to tune the position of λ_R with respect to the measurement wavelength. In this study, another measurement wavelength of 633 nm (λ_2) was used which was out of the resonance wavelength range of 650–736 nm.

MO properties of nanodisk arrays with various disk diameters measured at both 633 and 690 nm were summarized in Figs. 3(a) and 3(b). Both rotation angle and ellipticity at 633 nm showed monotonous dependence on disk diameter. At 690 nm, the rotation angle showed similar monotonous behavior, while ellipticity first increased and then decreased as increasing disk diameter and reached maximum for d of 84 nm as indicated by the arrow in Fig. 3(b). The monotonous size dependence can be attributed the fact that MO properties are proportional to the volume fraction (f) of MO materials when f is small. What is interesting is, the ellipticity at 690 nm showed peak value for moderate disk size. Moreover, nanodisk array corresponding to the peak ellipticity was associated with LSPR at this wavelength [see Fig. 2(b)], while λ_R for other disk sizes located on either the higher or lower energy side of this wavelength (690 nm). This result was consistent with the theoretical prediction[13] in 2007 that giant MO effect could be observed at LSPR resonance wavelength. Transmittance of nanodisk arrays at 690 nm was shown in Fig. 3(c). Both optical and MO properties at 690 nm were fitted in the framework of average field approximation,[15] where nanodisk array was approximated as a homogeneous slab with effective permittivity tensor and thickness. However, in this work, the authors will not present details about the modeling. To be noted is that, in expression (3.6a) of Ref. 15, permittivity of the host medium (noted as ε_1) and depolarization factor (noted as N) should be treated as fitting parameters. The deviation of ε_1 from its intrinsic value (~2.25) can be attributed mainly to the sidewall redeposits surrounding the nanodisk which was a mixture of metal atoms and organic materials produced during the etching process as shown in Fig. 1(b1). The array effect, i.e., the electric field of the nanodisk array acting on the surrounding dielectrics might also lead to enhanced electric polarization. However, this effect was not included in the Ref. 15. Since nanodisk consists of inhomogeneous materials, depolarization factor N depends not only on the shape but also compo-

sition, it is reasonable to treat this quantity as fitting parameter. The fitting results were shown in Figs. 3(a) and 3(c). Good agreement between experimental and fitting data was obtained. However, the authors would emphasize the importance of experimental data rather than the fitting one to support the conclusion in this work. That is, direct evidence for the correlation between enhancement of MO effect and excitation of LSPR was obtained.

To summarize, we presented the MO properties of nanodisk array with sandwich structure of $Au/[Co/Pt]_n/Au$ fabricated by EBL combined with argon ion milling. Excitation of LSPR was demonstrated for various disk diameters ranging from 53 to 119 nm. Resonance wavelengths were in the range of 650 to 736 nm accordingly and redshifted with increasing disk diameter. MO properties were obtained at wavelengths of 633 and 690 nm. Particularly, ellipticity measured at 690 nm first increased and then decreased with disk diameter and reached maximum for d of 84 nm, which was associated with LSPR at this wavelength. The results provide direct evidence for LSPR enhanced MO effect.

This work was partly supported by JSPS program of Postdoctoral Fellowship for Foreign researchers (Grant-in-Aid No. 2109282).

[1]A. B. Dahlin, J. O. Tegenfeldt, and F. Höök, Anal. Chem. **78**, 4416 (2006).
[2]P. H. Cheng, D. S. Li, Z. Z. Yuan, P. L. Chen, and D. R. Yang, Appl. Phys. Lett. **92**, 041119 (2008).
[3]F. J. García de Abajo, Rev. Mod. Phys. **79**, 1267 (2007).
[4]P. Neuzil and J. Reboud, Anal. Chem. **80**, 6100 (2008).
[5]J. H. Sung, B. S. Kim, C. H. Choi, M. W. Lee, S. G. Lee, S. G. Park, E. H. Lee, and O. B. Hoan, Microelectron. Eng. **86**, 1120 (2009).
[6]C. Hägglund, M. Zäch, and B. Kasemo, Appl. Phys. Lett. **92**, 013113 (2008).
[7]Y. Chen, K. Munechika, I. J. Plante, A. M. Munro, S. E. Skrabalak, Y. Xia, and D. S. Gingera, Appl. Phys. Lett. **93**, 053106 (2008).
[8]V. I. Safarov, V. A. Kosobukin, C. Hermann, G. Lampel, and J. Peretti, Phys. Rev. Lett. **73**, 3584 (1994).
[9]D. M. Newman, M. L. Wears, R. J. Matelon, and I. R. Hooper, J. Phys.: Condens. Matter **20**, 345230 (2008).
[10]J. B. González-Díaz, A. García-Martín, G. Armelles, J. M. García-Martín, C. Clavero, A. Cebollada, R. A. Lukaszew, J. R. Skuza, D. P. Kumah, and R. Clarke, Phys. Rev. B **76**, 153402 (2007).
[11]J. B. González-Díaz, A. García-Martín, J. M. García-Martín, A. Cebollada, G. Armellel, B. Sepúlveda, Y. Alaverdyan, and M. Käll, Small **4**, 202 (2008).
[12]P. K. Jain, Y. Xiao, R. Walsworth, and A. E. Cohen, Nano Lett. **9**, 1644 (2009).
[13]A. A. Zharov and V. V. Kurin, J. Appl. Phys. **102**, 123514 (2007).
[14]K. L. Kelly, E. Coronado, L. L. Zhao, and G. C. Schatz, J. Phys. Chem. B **107**, 668 (2003).
[15]M. Abe, Phys. Rev. B **53**, 7065 (1996).